

Article

A Non-Destructive Measurement Approach for the Internal Temperature of Shiitake Mushroom Sticks Based on a Data–Physics Hybrid-Driven Model

Xin Zhang ¹, Xinwen Zeng ^{1,2}, Yibo Wei ^{3,4}, Wengang Zheng ^{3,4} and Mingfei Wang ^{3,4,*}

¹ College of Mechanical and Electrical Engineering, Xinjiang Agricultural University, Urumqi 830052, China; zhangx@nercita.org.cn (X.Z.); mingfeiwang3@outlook.com (X.Z.)

² Xinjiang Intelligent Agricultural Machinery Equipment Engineering Technology Center, Urumqi 830052, China

³ Intelligent Equipment Technology Research Center, Beijing Academy of Agriculture and Forestry Sciences, Beijing 100097, China; weiyb@nercita.org.cn (Y.W.); kongxs@nercita.org.cn (W.Z.)

⁴ Information Technology Research Center, Beijing Academy of Agriculture and Forestry Sciences, Beijing 100097, China

* Correspondence: wangmf@nercita.org.cn

Abstract: This study aimed to develop a non-destructive measurement method utilizing acoustic sensors for the efficient determination of the internal temperature of shiitake mushroom sticks during the cultivation period. In this research, the sound speed, air temperature, and moisture content of the mushroom sticks were employed as model inputs, while the temperature of the mushroom sticks served as the model output. A data–physics hybrid-driven model for temperature measurement based on XGBoost was constructed by integrating monotonicity constraints between the temperature of the mushroom sticks and sound speed, along with the condition that limited the difference between air temperature and stick temperature to less than 2 °C. The experimental results indicated that the optimal eigenfrequency for applying this model was 850 Hz, the optimal distance between the sound source and the shiitake mushroom sticks was 8.7 cm, and the temperature measurement accuracy was highest when the moisture content of the shiitake mushroom sticks was in the range of 56–66%. Compared to purely data-driven models, our proposed model demonstrated significant improvements in performance; specifically, RMSE, MAE, and MAPE decreased by 74.86%, 77.22%, and 69.30%, respectively, while R² increased by 1.86%. The introduction of physical knowledge constraints has notably enhanced key performance metrics in machine learning-based acoustic thermometry, facilitating efficient, accurate, rapid, and non-destructive measurements of internal temperatures in shiitake mushroom sticks.

Keywords: shiitake mushroom stick; acoustic thermometry; data–physics hybrid; non-destructive measurement



Citation: Zhang, X.; Zeng, X.; Wei, Y.; Zheng, W.; Wang, M. A Non-Destructive Measurement Approach for the Internal Temperature of Shiitake Mushroom Sticks Based on a Data–Physics Hybrid-Driven Model. *Agriculture* **2024**, *14*, 1841. <https://doi.org/10.3390/agriculture14101841>

Academic Editor: Bruno Bernardi

Received: 14 September 2024

Revised: 10 October 2024

Accepted: 17 October 2024

Published: 18 October 2024



Copyright: © 2024 by the authors. Licensee MDPI, Basel, Switzerland. This article is an open access article distributed under the terms and conditions of the Creative Commons Attribution (CC BY) license (<https://creativecommons.org/licenses/by/4.0/>).

1. Introduction

Edible fungi are found to hold a crucial role in global agricultural products, of which the shiitake mushroom is one of the main varieties. Its cultivation area is vast, and the annual production and consumption of shiitake mushrooms are reported to occupy an important position in global edible fungi products [1]. Mycelial physiological maturity is referred to as the stage after the Shiitake mushroom mycelium has grown all over the stick and before it moves to the mushroom shed. The accurate judgment of mycelial maturity is considered crucial during cultivation, as it is believed to directly affect the yield and quality of the shiitake mushroom [2]. Currently, the mycelium is usually assessed for maturity using the accumulated temperature method [3], but mushroom farmers often use air temperature or the surface temperature of the mycelium stick instead of the internal

temperature, which leads to a significant measurement error and misses the optimal mushrooming time. The method of temperature detection using a metal probe is limited in its ability to accurately reflect the internal temperature range of mycelium and disrupts the growth microenvironment, which is detrimental to mycelial cultivation processes. Common non-destructive temperature measurement techniques primarily include acoustic thermometry and infrared thermography [4]; however, infrared thermography typically only measures surface temperatures and fails to provide insights into the internal temperature of mycelium. Consequently, there is an urgent need identified for a non-destructive and efficient method to measure the internal temperature of mycorrhizal rods for assessing mycelial maturity, in conjunction with the cumulative temperature method.

Acoustic thermometry is a non-invasive and reliable temperature measurement method that indirectly measures temperature by using the corresponding relationship between the speed of sound propagation in the medium and the temperature [5]. It not only protects the structure of the shiitake mushroom sticks and the bacterial environment but also has the advantages of being fast, accurate, and non-contact [6], making it the best way to detect the temperature of the ingredients inside the shiitake mushroom sticks.

Acoustic thermometry has found wide applications in various fields, such as grain temperature monitoring [7–9], biomass fuel temperature detection [10,11], and air temperature field analysis [12,13]. Yan et al. employed an experimental calibration method to establish the physical relationship between sound velocity and temperature within the stacked structure of biomass materials, thereby validating the feasibility of acoustic thermometry for use in these materials [14]. Guo et al. experimentally verified a single-path acoustic temperature measurement method for wood pellet piled structures and proposed a non-invasive approach based on acoustic sensing technology using low-frequency sound waves and cross-correlation processing techniques to measure the temperature of stored biomass. Their experiments demonstrated effective temperature measurements for wood materials within the range of 22~48.9 °C [15]. Holstein et al. utilized cross-correlation methods to calculate the average sound speed along sound wave propagation paths, effectively eliminating the influence of air flow speed on measured sound velocity fields [16]. Bao et al. performed simultaneous acoustic signal transmission and acoustic wave transit time measurements for multiple acoustic paths, followed by air temperature field reconstruction using an offline iterative algorithm, which shortened the computation time and achieved high accuracy in temperature field reconstruction [17].

The relationship between the internal sound speed and temperature in the medium was the result of the combined effects of multiple factors, including the moisture content of the medium, the temperature difference between the inside and outside of the medium, and the distribution of the sound source and medium. To solve the problem of the complex interaction of multiple factors affecting the accurate and rapid monitoring of temperature fields, Lin et al. proposed a machine learning method based on convolutional neural networks (CNNs) to reconstruct the gas temperature distribution (TD) from the sound speed, which improved the 2D visualization results, indicating that machine learning methods can be applied in complex relationships between sound speed and medium temperature [18]. Zhong et al. proposed a machine learning approach for reconstructing the temperature field in acoustic thermometry based on the Kernel Extreme Learning Machine (KELM), which enhances both the speed of the temperature computation and the computational accuracy [19]. Jeong et al. proposed and successfully proved a machine learning-based method for obtaining the transit time measurement model and estimating the temperature distribution [20]. Ma et al. used a CDMA-based acoustic signal modulation technique to improve the Signal-to-Interference-plus-Noise Ratio and established a kernel regression model with spatially dependent Gaussian radial basis function and time-dependent coefficients. The Gaussian function parameters were optimally solved by gradient descent, and the numerical simulation shows that the error of 3D temperature field reconstruction was less than 5%, which verifies the feasibility and high efficiency of the machine learning method in measuring temperature using the speed of sound [21].

XGBoost (eXtreme Gradient Boosting) has integrated multiple decision trees, offering a novel approach to enhance the accuracy of temperature measurements under conditions characterized by multi-factor coupling. Jeon et al. developed a machine learning-based model to predict the internal environment of greenhouses cultivating melons. This model effectively captured the complex inter-relationships among greenhouse environmental factors and successfully established a monitoring framework for melon cultivation environments [22]. Tang et al.'s comparative analysis was conducted involving several mainstream single model algorithms, including XGBoost, as well as integrated learning algorithms, to validate the superiority of XGBoost's integrated learning capabilities [23]. Weierbach et al. found that the combined model integrated with XGBoost was significantly better than other ensemble models in measuring river temperatures [24]. Yang et al. conducted a comparative analysis of four models—Support Vector Regression (SVR), Random Forest Regression (RFR), Multi-Layer Perceptron (MLP), and XGBoost utilizing the same dataset; the XGBoost model consistently surpassed the performance of the other three models [25]. Consequently, XGBoost has been found to be particularly well suited for scenarios characterized by abundant data and complex challenges, enabling rapid and reliable high-quality measurements [22].

When employing the XGBoost model to measure temperature changes within the medium, the black box nature of purely data-driven models complicates the interpretation of their internal decision-making processes, leading to suboptimal temperature measurement. In contrast, the data-physics hybrid-driven model integrates the benefits of prior knowledge with data-driven methods, enhancing both model interpretability and measurement accuracy [26,27].

This paper proposed a non-destructive method for measuring the internal temperature of shiitake mushroom sticks using microphones. The method combines machine learning and physical knowledge to construct a model for measuring the internal temperature of shiitake mushroom sticks. The study first collected a large dataset covering the influence of factors such as different air temperatures, moisture contents of the shiitake mushroom stick, temperatures of the shiitake mushroom stick, and frequencies of different sound sources. These datasets were used for the training and validation of the XGBoost model. Furthermore, this study incorporates physical constraints into the model training process, including the frequency characteristics of acoustic signal propagation within shiitake mushroom sticks and the monotonic relationship between sound velocity and temperature in these sticks, resulting in a data-physics hybrid-driven XGBoost model. Finally, the temperature measurement effect of the purely data-driven model and the data-physics hybrid-driven model was verified and evaluated separately. This study will provide a novel, non-invasive solution for the internal temperature detection of shiitake mushroom sticks, enabling its non-destructive measurement.

This paper investigates the non-destructive measurement of internal temperature in shiitake mushroom sticks, structured into five sections: Section 1 introduces the significance of non-destructive temperature estimation for shiitake mushroom sticks and provides relevant technological background; Section 2 outlines the principles of acoustic temperature estimation, detailing the experimental design, data acquisition process, and construction of a temperature estimation model; Section 3 analyzes various factors influencing model performance and compares these results with those from other models; Section 4 discusses the feasibility of this method in cultivating other edible fungi species as well as its application in shiitake greenhouse cultivation. Finally, Section 5 summarizes the key research findings.

2. Materials and Methods

2.1. Acoustic Wave-Based Non-Destructive Temperature Measurement for Shiitake Mushroom Sticks

Acoustic temperature measurement relies on the correlation between sound speed and temperature within a given medium. The speed of sound was the most critical intermediate quantity in the acoustic temperature measurement process, but the speed of sound was

affected by the frequency of the sound wave, the moisture content of the shiitake mushroom stick, the air temperature, and the distance from the sound source. Given that the moisture of air in the bacterial cultivation room remained exceptionally stable, its impact on sound velocity was relatively minor compared to other factors mentioned above. Consequently, the influence of air humidity on sound velocity was not considered during the initial model development and training process.

The low thermal conductivity coefficient of the shiitake mushroom stick material led to a gradual temperature variation, while the specific heat capacity of air was also relatively low. This facilitated rapid heat exchange and thermal equilibrium between the air within the shiitake mushroom stick and the mushroom material. Consequently, the temperature fluctuation of the air in the interstitial spaces could be considered equivalent to that of the shiitake mushroom sticks themselves.

Guo et al. proposed a non-invasive temperature measurement method utilizing microphone technology. This approach involved measuring the temperature within biomass accumulation structures through low-frequency sound waves and cross-correlation processing techniques. The findings indicated that the accuracy of measuring the transit time of sound wave signals, particularly at characteristic frequencies ranging from 600 Hz~1 kHz, was significantly enhanced when employing the cross-correlation method [15]. The cross-correlation method determined the time delay between two microphones by utilizing the time delay t as the transit duration of the acoustic signal within the shiitake mushroom stick. This method was predicated on the waveform similarity of the signals, where the actual time delay was identified as the interval at which two signals exhibited maximum correlation. Let us denote $f_1(x)$ and $f_2(x)$ as time-domain acoustic signals with a specific temporal gap; thus, their cross-correlation function could be expressed in Equation (1).

$$R_{12}(m) = \frac{\sum_{t=1}^{N-M} f_1(t)f_2(t+m)}{\sqrt{\sum_{t=1}^{N-M} f_1^2(t)}\sqrt{\sum_{t=1}^{N-M} f_2^2(t)}}, 0 \leq m \leq M \quad (1)$$

where $f_1(t)$ and $f_2(t)$ denote the sampled values of the signals $f_1(x)$ and $f_2(x)$, respectively; N denotes the total number of data points in the sampled signals; m denotes the number of delayed sampling points ($m = 0, 1, 2, \dots, h, \dots, M$). Here, M represents the number of samples used for calculating the cross-correlation function at maximum allowable delay. The peak value of the function $R_{12}(m)$, known as the cross-correlation coefficient, quantifies the degree of similarity between two sound signals. The transit time of the sound signal is calculated using Equation (2).

$$t = h * \Delta t \quad (2)$$

where t denotes the transit time of the acoustic signal; h denotes the abscissa corresponding to the maximum value of $R_{12}(m)$ in the range 0 to M ; Δt denotes the time interval between signal acquisitions. The velocity of the acoustic signal is calculated from Equation (3).

$$C = \frac{d}{t} \quad (3)$$

where C denotes the velocity of the acoustic wave; d is the distance between the microphones; t is the acoustic wave transit time.

This study employed low-frequency acoustic waves to measure the internal temperature of mycelium sticks; however, the microphone configuration differed from that in reference [15]. In reference [15], all the microphones were embedded within the medium, which compromised the structural integrity of its edges. The layout is illustrated in Figure 1. Conversely, this study aimed to achieve a non-destructive measurement of temperature within the mycelium stick. To preserve the internal microenvironment, the microphones were positioned on both sides of the measuring medium, as depicted in Figure 2. Furthermore, compared to the literature [15], this paper must also consider the phenomenon of low-frequency acoustic wave bypassing [28–30].

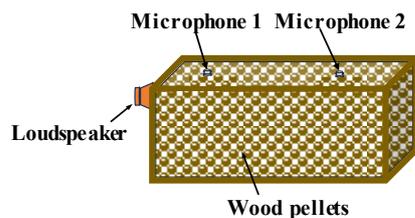


Figure 1. Microphone placement as reported in the literature [15].

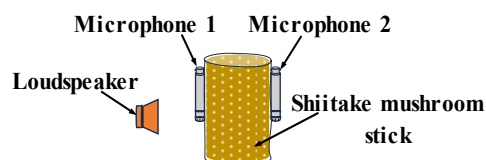


Figure 2. Microphone placement in this study.

In this study, the acoustic wave signals received by microphone 1 indicated signals that were about to be incident on the shiitake mushroom stick, which was different from the signals received by microphone 1 in the literature [15] that had already entered the medium. The signal received by microphone 2 consisted of an acoustic signal that penetrated the shiitake mushroom stick to the air and an acoustic signal that was projected around along the surface of the shiitake mushroom stick, which was different from the literature [15], where microphone 2 was in the medium, and only the signal that penetrated the medium was captured.

2.2. Experimental Materials

2.2.1. Mushroom Stick Material

In this study, the short shiitake mushroom sticks randomly selected from the production line of factory-cultivated shiitake mushrooms at the germination stage were subjected to experimental measurements (Figure 3). The material composition ratio of the short shiitake mushroom stick comprised 78% wood shavings, 20% bran, 1% lime, and 1% gypsum, with moisture content ranging from 45~77%. The short shiitake mushroom stick was mixed and filled using automated production equipment to ensure uniform particle distribution and regular shape, then wrapped in a double-layer high-density polyethylene plastic bag, with inner and outer bag thicknesses of 0.01 mm and 0.05 mm, respectively. The diameter of the shiitake mushroom stick was measured at 10.5 cm, while their height was recorded as 20 cm. The center of the shiitake mushroom stick was selected for experimental data collection. They were then externally wrapped in double-layer high-density polyethylene plastic bags, with inner and outer bag thicknesses measuring 0.01 mm and 0.05 mm, respectively. The diameter of the shiitake mushroom stick was measured as $d = 10.5$ cm, while their height was recorded at $h = 20$ cm. The central region of the shiitake mushroom stick was selected for the experiment, during which the data on sound velocity and temperature were collected.



Figure 3. Shiitake mushroom sticks used in the experiment.

2.2.2. Data Acquisition System

The composition of the measurement system is illustrated in Figure 4. The self-developed LabVIEW computer software V1.1 controlled the NI acquisition card to generate acoustic signals of the desired frequency and duration. These signals were linearly amplified by a power amplifier, which drove a low-frequency loudspeaker to emit a sinusoidal wave lasting 100 ms, starting at a frequency of 600 Hz and increasing in steps of 50 Hz up to a cutoff frequency of 1 kHz.

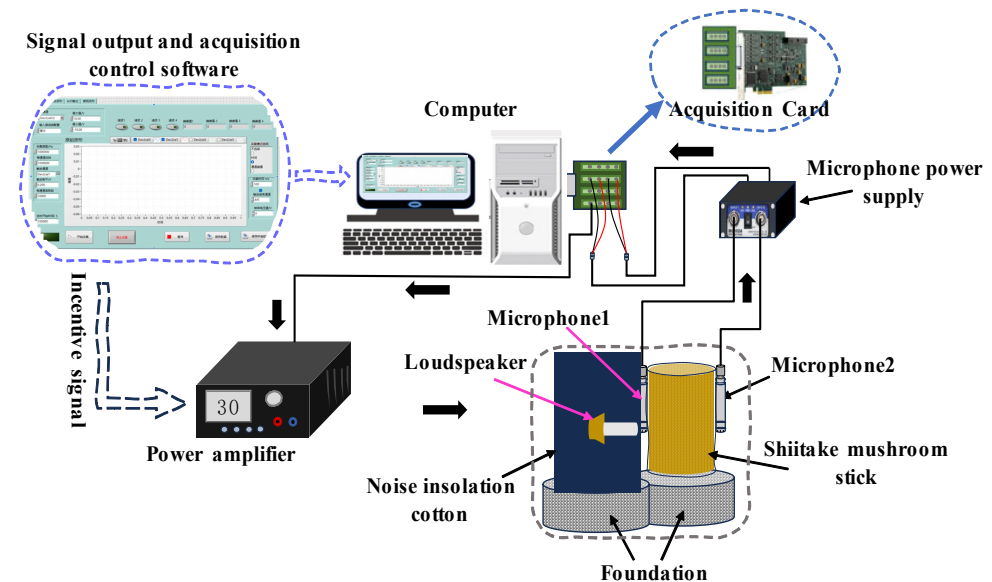


Figure 4. Schematic diagram of sound velocity measurement system connection and the velocity of the composite acoustic signal measurement.

As illustrated in Figure 4, the microphones and speakers positioned on both sides of the shiitake mushroom sticks were aligned horizontally. The signal received by microphone 1 consisted of the incident signal from the front surface of the shiitake mushroom stick combined with noise, while microphone 2 captured a composite acoustic signal along with noise. This composite acoustic signal was formed by superimposing the penetrating acoustic signal from the shiitake mushroom stick and an additional acoustic signal transmitted along their surface. Subsequently, host computer software controlled the NI acquisition card to save signals received by both microphones for a duration of 100 ms. In this study, a bandpass filtering algorithm was employed to reduce noise in these signals, followed by using mutual correlation methods to calculate the time delay between the incident and composite signals; finally, the velocity of the composite acoustic signal was determined using Equation (3). The operating steps of the complete collection system are shown in Figure 5.

In the measurement system of this study, the microphone utilized was a model MPA265 from Beijing Soundwatch (BSWA) Technology Co., Ltd. (Beijing, China) featuring a response frequency range of 20 Hz~12.5 kHz. The power amplifier used in this study was the model ATA-2021B from Xi'an Aigtek Electronic Technology Co., Ltd. (Xi'an, China), with a maximum output power of 50 W. The loudspeaker was obtained from Dongguan Guanyin Audio Co., Ltd. (Dongguan, China), model YD78DQTZF-01, with a rated power of 15 w, a resistance value of 8 Ω , and a frequency response range of 108 Hz~20 kHz. The data acquisition card used was the NI-PCIe-6374 high-speed data acquisition card from National Instruments (NI) Co., Ltd. (Austin, TX, USA), which features a 4-channel analog input, a 2-channel analog output, and a 16-bit resolution with a maximum sampling rate of 3.57 MS/s. According to the experimental requirements, based on LabVIEW language development contains signal modulation, signal acquisition, and other functions in one of the acquisition card control software. The constant temperature and humidity test

chamber used in the experiment was produced by Guangdong Xingtuo Environmental Test Equipment Technology Co., Ltd. (Dongguan, China), model AH-408, with temperature control accuracy of ± 0.5 °C and humidity control accuracy of $\pm 2.5\%$ RH. The digital temperature inspection instrument used in this experiment was manufactured by Pumei Instruments (Zhongshan) Co., Ltd. (Zhongshan, China), specifically the 8-channel model DC700. The temperature probe was custom designed by (RTHOYE) Shenzhen Rongtai Hongye Technology Co., Ltd. (Shenzhen, China) and features a length of 3.5 cm. When used in conjunction with the digital thermometer, the temperature measurement accuracy is ± 0.02 °C.

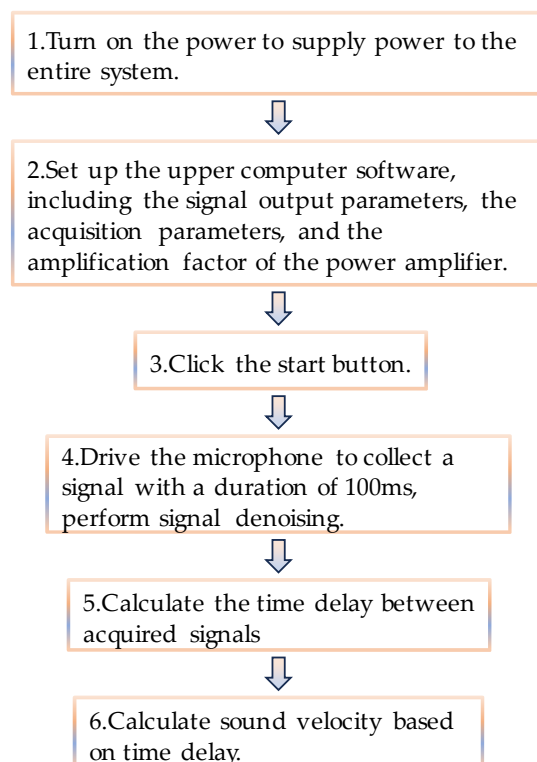


Figure 5. Operation steps of the sound velocity measurement system.

In this study, a moving coil loudspeaker was employed as the sound source. The resulting acoustic signal was unfocused, leading to a low Signal-to-Interference-plus-Noise Ratio (SINR) in the acquired data. To address this issue, sound insulation cotton was utilized to modify the sound source prior to the experiment. The acoustic insulation properties of the material effectively concentrated the acoustic signal along the central axis of the loudspeaker's propagation path.

To measure the velocity and amplitude of the penetrating acoustic signal within the shiitake mushroom stick, modifications to the arrangement of microphones depicted in the dotted box of Figure 4 were required, as illustrated in Figure 6. Within a constant temperature and humidity experimental chamber, there existed a minimal gap between Microphone 1 and the surface of the shiitake mushroom stick, while Microphone 2 was positioned inside the stick. Both microphones were aligned along the same horizontal axis. Additionally, an electronic thermometer probe was placed at every 90° interval within the middle section of the shiitake mushroom stick to monitor temperature variations. Each probe had an insertion depth of 4 cm.

As illustrated in Figure 6, the two microphones were positioned inside and outside the shiitake mushroom sticks and were aligned horizontally with the loudspeaker. The signal was received by microphone 1, which consisted of a combination of the incident signal and noise from the front surface of shiitake mushroom sticks, while microphone 2 captured a mixture of penetrating acoustic signals and noise. Subsequently, host computer

software controlled the NI acquisition card to save signals acquired by both microphones for a duration of 100 ms. After applying bandpass filtering and noise reduction to these signals, cross-correlation methods were employed to calculate the time delay between the incident signal and penetrating acoustic signal; finally, the velocity of the penetrating acoustic signal was determined using Equation (3).

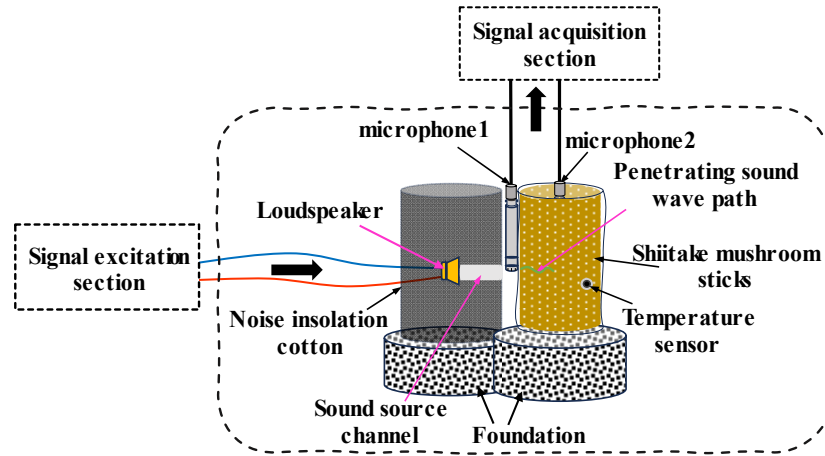


Figure 6. Schematic diagram for measuring the velocity of the penetrating acoustic signal inside the shiitake mushroom stick.

2.3. Data Collection

2.3.1. Sound Velocity Data at Different Acoustic Frequencies

In this study, the velocities of the composite acoustic signal C_{1i} and the penetrating acoustic signal C_{2i} were measured within the shiitake mushroom stick for signals in the frequency range of 600 Hz~1 kHz, with results presented in Figure 7. The temperature T of the shiitake mushroom sticks during experimentation was recorded at 22.4 °C, while the moisture content of the mushroom stick was determined to be 66.47%. Additionally, the ambient air temperature T_k surrounding the shiitake mushroom stick was measured at 23.4 °C, and relative humidity levels were found to be 75.3%. When discrepancies among measurements from four material temperature sensors did not exceed 0.1 °C, their average value was utilized to represent the temperature T of the shiitake mushroom stick.

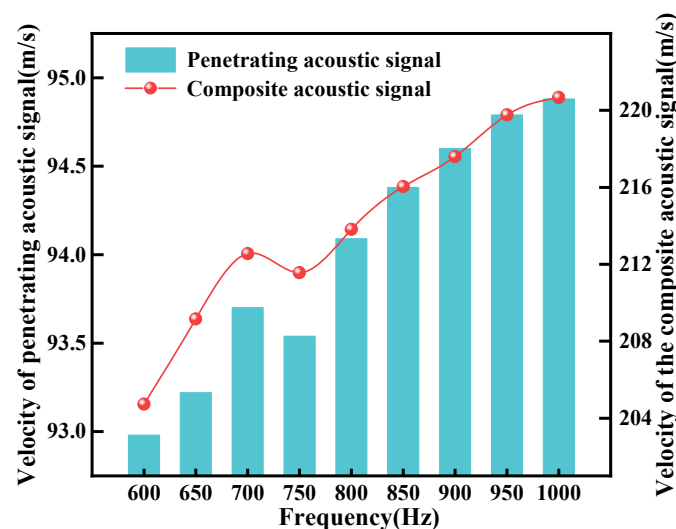


Figure 7. Velocity of the composite acoustic signal and velocity of penetrating acoustic signal at different frequencies.

The signal frequency ranged from 600 Hz~1 kHz, and both the velocity of the penetrating acoustic signal and the velocity of the composite acoustic signal increased with the frequency. This was due to the dispersion phenomenon of sound waves in the material [31]. Acoustic signals propagated through the air gap within the shiitake mushroom sticks; however, the velocities of the composite acoustic signal and the penetrating acoustic signal were remarkably lower than that of sound in free-field air. This was attributed to the complex structure within the shiitake mushroom sticks, which caused sound waves to undergo multiple reflections and scattering. Additionally, the material of the shiitake mushroom sticks exhibited a certain degree of absorption for acoustic signals, resulting in an acoustic impedance that was higher than that of air.

Remarkably, the scattering of acoustic signals occurred when biomass materials were employed as the medium. To further identify the optimal characteristic frequency point, this study measured the sound pressure amplitude of penetrating acoustic signals at various frequencies within shiitake mushroom sticks. The sound pressure amplitude was determined by calculating the average amplitude of the signal collected from within the stick. The calculation formula is presented in Equation (4).

$$L = 20 \log_{10} \left(\frac{V_1}{V_0} \right) \quad (4)$$

where L represents the sound pressure amplitude in units of dBuV; V_1 denotes the measured voltage amplitude in units of μV ; and V_0 refers to the reference voltage in units of $1 \mu\text{V}$. The experimental results are shown in Figure 8.

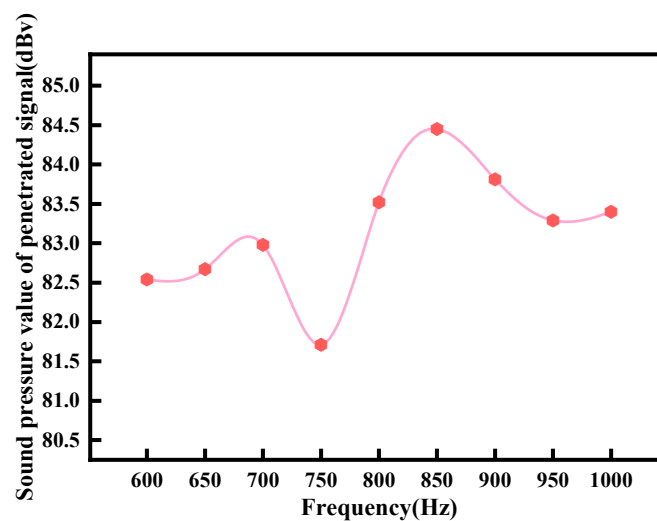


Figure 8. Sound pressure amplitude of penetrating acoustic signal at different frequencies.

The amplitude of acoustic pressure was maximized for signals at a frequency of 850 Hz, while that for signals at 750 Hz was minimized. This indicates that the shiitake mushroom stick exhibited minimum acoustic impedance to 850 Hz signals and maximum acoustic impedance to 750 Hz signals.

In this study, the velocity of the composite acoustic signal with the temperature T of the shiitake mushroom stick was measured in the frequency range of 600 Hz~1 kHz, and the results are shown in Figure 9.

Within the temperature range of 18~42 °C for shiitake mushroom sticks, the velocity of the composite acoustic signal in the frequency range of 600 Hz~1 kHz was found to consistently increase with rising temperature. As the temperature of the shiitake mushroom sticks was elevated, the rate of change in sound velocity per unit temperature at each frequency was found to gradually intensify. The minimum change in sound velocity per unit temperature for an 850 Hz sound wave signal was measured at 0.41 m/s, which outperformed that observed at other frequencies. Consequently, when utilizing a frequency

of 850 Hz, temperature measurement was able to achieve the highest resolution, and the sound impedance of shiitake mushroom sticks to 850 Hz waves was minimized. Therefore, this study selected a sound wave signal frequency of 850 Hz.

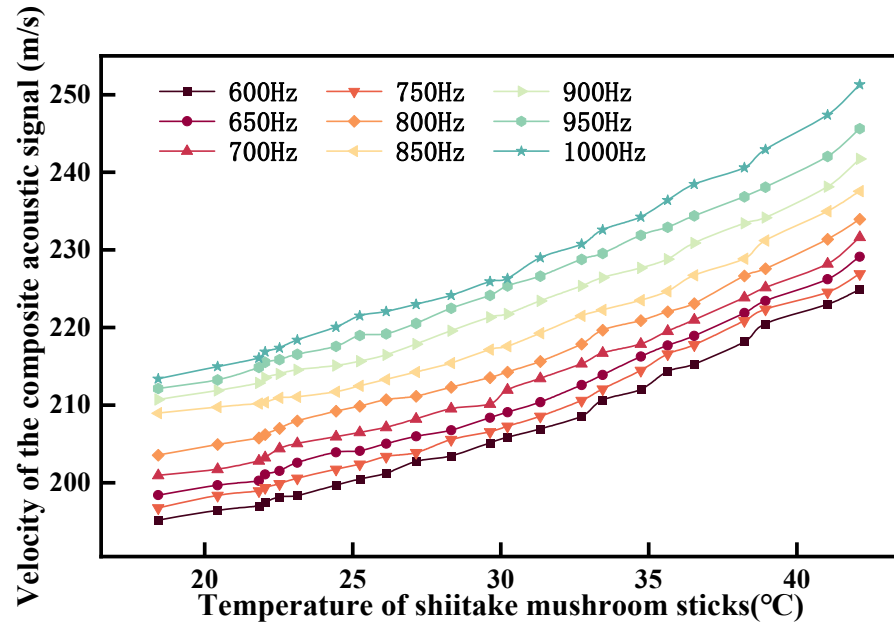


Figure 9. Variation of composite acoustic signal velocity across different acoustic wave frequencies in the temperature range.

2.3.2. Sound Velocity Data at Different Moisture Contents of Shiitake Mushroom Sticks

In order to measure the velocity of the penetrating acoustic signal and the composite acoustic signal of the shiitake mushroom sticks, the moisture content of the sticks was set in the range of 45~77% under the conditions of 22.4 °C temperature of the sticks and 22.2 °C temperature of the air around the sticks. The measurement results are shown in Figure 10.

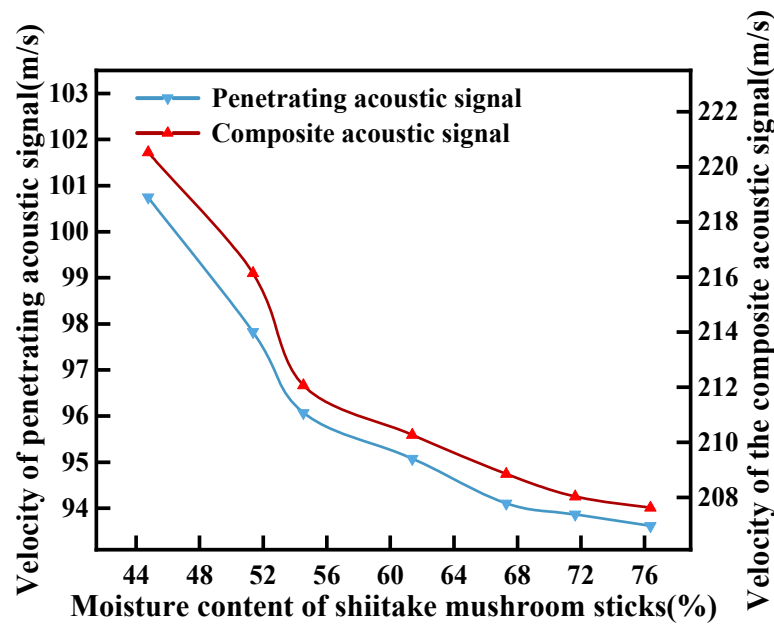


Figure 10. Variation of velocity of penetrating acoustic signal and composite acoustic signal at different moisture contents of shiitake mushroom sticks.

The velocities of both the composite acoustic signal and the penetrating acoustic signal were found to exhibit a decline with increasing moisture content in shiitake mushroom sticks. For moisture content of 45~55% of the shiitake mushroom sticks, the rate of change in the velocity of the composite acoustic signal C_{1i} was measured at 3.836%, and the rate of change in the velocity of penetrating acoustic signal C_{2i} was measured at 4.676%. For moisture content of 56~66% of the shiitake mushroom sticks, the rate of change in the velocity of the composite acoustic signal C_{1i} was measured at 1.99%, and the rate of change in the velocity of penetrating acoustic signal C_{2i} was measured at 2.4%, which was smaller than the rate of change in the range of 45~55%. When the moisture content of the shiitake mushroom sticks was in the range of 67~77%, the rate of change in the velocity of the composite acoustic signal C_{1i} was measured at 0.317%, and the rate of change in the velocity of the penetrating acoustic signal C_{2i} was measured at 0.516%.

The increase in moisture content was found to lead to a decrease in both the velocity of the composite acoustic signal and the velocity of the penetrating acoustic signal. Both were attributed to the fact that the increase in the moisture content of the shiitake mushroom sticks hindered the propagation of the penetrating acoustic signal. Consequently, the ratio of the decrease in velocity for the penetrating acoustic signal to that for the composite acoustic signal could be interpreted as representing the proportion of the penetrating acoustic signal within the composite acoustic signal. When moisture contents of shiitake mushroom sticks were within ranges of 45~55%, 56~66%, and 66~77%, the corresponding proportions of penetrating acoustic signals were measured at 55.3%, 61.1%, and 39.51%, respectively. The optimal moisture content for shiitake mushroom mycelium growth was reported to be between 60% and 65% [32]. Within this range, the proportion of penetrating acoustic signals relative to composite signals was maximized, facilitating accurate transit time calculations.

2.3.3. Velocity of Sound Data at Different Temperatures

To measure the velocity of the composite acoustic signal at varying temperatures of both the air and shiitake mushroom sticks, the air temperature was maintained within a range of 18~42 °C, while the moisture content of the shiitake mushroom sticks was set at 65.28%, and the air humidity was set at 75.36%. The relationship between the velocity of the composite acoustic signal and the temperature of the shiitake mushroom sticks is shown in Figure 11a, whereas Figure 11b depicts how this velocity varies with changes in air temperature.

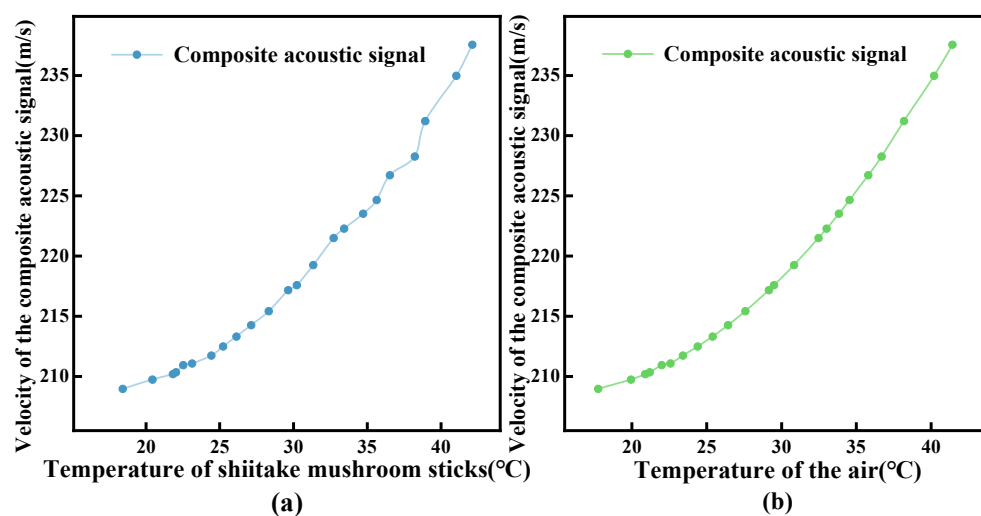


Figure 11. Variation of composite acoustic signal velocity with shiitake mushroom stick temperature and air temperature. (a) Variation of the velocities of the composite acoustic signal with the temperature of the shiitake mushroom sticks; (b) Variation of the velocities of the composite acoustic signal with the temperature of the air surrounding the shiitake mushroom sticks.

The experimental results indicated that the velocity of the composite acoustic signal C_{1i} increased with the temperature of the shiitake mushroom sticks, demonstrating a monotonically increasing relationship between C_{1i} and the temperature of the shiitake mushroom sticks. Additionally, the velocity of C_{1i} also rose with an increase in air temperature, exhibiting a similar monotonically increasing relationship between C_{1i} and air temperature.

2.4. Temperature Measurement Models and Evaluation Metrics

2.4.1. Temperature Measurement Model Construction

In this study, the XGBoost model was selected for data–physics hybrid modeling. The model utilized the moisture content of the shiitake mushroom sticks, the velocity of the composite acoustic signal, and air temperature as input features, with the internal temperature of the shiitake mushroom sticks used as the output variable. The dataset was divided into training, validation, and test sets in a ratio of 6:2:2.

During the data preprocessing stage, the velocity of the composite acoustic signal was observed to exhibit fluctuations due to interference from various noise sources. Nevertheless, given the established monotonically increasing relationship between velocity and air temperature, as well as the monotonically decreasing relationship between velocity and moisture content of shiitake mushroom sticks, this study employed these relationships to identify and filter out anomalous data points.

This study employed the XGBoost algorithm for temperature prediction, with the model articulated as follows:

$$\hat{T}_i(x) = \beta_0 + \beta_1 x_1 + \beta_2 x_1^2 + \beta_3 x_1^3 + \beta_4 x_2 + \beta_5 x_3 + \beta_6 (x_1 \cdot x_2) + \beta_7 (x_1^2 \cdot x_2) \quad (5)$$

where x_1 denotes the velocities of the composite acoustic signal; x_2 indicates the moisture content of the shiitake mushroom stick; and x_3 represents the air temperature. The parameters $\beta_0, \beta_1, \dots, \beta_6$, and β_7 signify the influence weights of each input factor on the output results. This study employs a non-negative least squares method to estimate parameter β . The optimized objective function is presented in Equation (6).

$$\min \sum_{i=1}^n (y_i - \hat{T}(x_i; \beta))^2 \quad (6)$$

To ensure that the temperature prediction function $\hat{T}_i(x)$ adhered to the monotonically increasing constraints between the velocities of the composite acoustic signal and the temperature of the shiitake mushroom sticks, it was essential to satisfy the following conditions:

$$\frac{\partial \hat{T}_i(x)}{\partial x_1} = \beta_1 + 2\beta_2 x_1 + 3\beta_3 x_1^2 + \beta_6 x_2 + 2\beta_7 x_1 x_2 \geq 0 \quad (7)$$

In this study, the XGBoost package (version 1.5.2) was implemented in Python and was utilized, with parameters such as monotonic constraints configured accordingly. Furthermore, the loss function of the XGBoost model is represented by Equation (8).

$$L(\hat{T}_i, T_i) = \frac{1}{n} \sum_{i=1}^n (\hat{T}_i - T_i)^2 \quad (8)$$

where \hat{T}_i denotes the model measurement of shiitake mushroom stick temperature values; T_i denotes the sensor measurement of shiitake mushroom stick temperature values.

Additionally, it was empirically observed that the temperature of shiitake mushroom sticks typically did not exceed 2 °C above the surrounding air temperature. Consequently, this constraint is incorporated into the monotonicity constraints. The updated loss function could be expressed as shown in Equation (9).

$$L'(\hat{T}_i, T_i, T_k) = L(\hat{T}_i, T_i) + \alpha * \text{penalty}(|\hat{T}_i - T_k| - 2) \quad (9)$$

where \hat{T}_i is the measured temperature of the shiitake mushroom sticks; T_i is the actual temperature of the shiitake mushroom sticks; T_k is the air temperature; α is a hyperparameter that controls the strength of the penalty, with values ranging from 0~1; and $\text{penalty}(x)$ is a penalty function, and its form is presented in Equation (10).

$$\text{penalty}(x) = \begin{cases} 0 & \text{if } x \leq 0 \\ x & \text{if } x > 0 \end{cases} \quad (10)$$

2.4.2. Model Assessment Indicators

The computer hardware and software utilized in the experiment were as follows: the CPU processor was an Intel i7-12700H with 16 GB of RAM (Intel, Santa Clara, CA, USA); the GPU graphics card was an NVIDIA RTX 3060 (NVIDIA, Santa Clara, CA, USA); the operating system was 64-bit Windows 11; the programming environment was Python 3.6; and the integrated development environment used was PyCharm Community Edition 2022.3.2.

To assess the performance of the model, this study employed root mean square error (RMSE), mean absolute error (MAE), mean absolute percentage error (MAPE), and the coefficient of determination (R^2) as assessment indicators.

$$\text{RMSE} = \sqrt{\frac{1}{n} \sum_{i=1}^n (y_i - \hat{y}_i)^2} \quad (11)$$

$$\text{MAE} = \frac{1}{n} \sum_{i=1}^n |y_i - \hat{y}_i| \quad (12)$$

$$\text{MAPE} = \frac{100\%}{n} \sum_{i=1}^n \left| \frac{y_i - \hat{y}_i}{y_i} \right| \quad (13)$$

$$R^2 = 1 - \frac{\sum_{i=1}^n (y_i - \hat{y}_i)^2}{\sum_{i=1}^n (y_i - \bar{y}_i)^2} \quad (14)$$

where y_i denotes the sensor measurement of shiitake mushroom stick temperature values; \bar{y}_i denotes the average of the sensor measurement of shiitake mushroom stick temperature values; \hat{y}_i denotes the model measurement of shiitake mushroom stick temperature values.

3. Results

3.1. The Influence of Acoustic Frequency on Temperature Measurement Effect

To identify the best characteristic frequency for measuring the temperature of shiitake mushroom sticks, this study employed different frequencies of sound waves for testing and verification. The effect of measuring the temperature of the shiitake mushroom sticks based on the data–physics hybrid drive temperature measurement model is shown in Table 1.

Table 1. Evaluation metrics for data–physics hybrid drive models at various frequencies.

Frequency (Hz)	RMSE (°C)	MAE (°C)	MAPE (%)	R^2
600	0.092	0.083	0.295	0.991
650	0.082	0.088	0.277	0.995
700	0.088	0.079	0.279	0.993
750	0.130	0.113	0.385	0.988
800	0.083	0.079	0.273	0.994
850	0.054	0.047	0.218	0.999
900	0.087	0.081	0.291	0.994
950	0.081	0.075	0.276	0.996
1000	0.082	0.079	0.281	0.992

The temperature measurement model exhibited an RMSE of 0.054 °C, a MAE of 0.047 °C, a MAPE of 0.218%, and an R^2 of 0.999 for the acoustic wave frequency of 850 Hz. At an acoustic frequency of 750 Hz, the temperature measurement model demonstrated an RMSE of 0.13 °C, a MAE of 0.113 °C, a MAPE of 0.385%, and an R^2 value of 0.988. In comparison to the measurements at this frequency, the RMSE, MAE, and MAPE for the temperature measurement model at an acoustic frequency of 850 Hz decreased by approximately 58.5%, 58.4%, and 43.4%, respectively; additionally, R^2 had improved by about 1.12%.

According to the RMSE, MAE, and MAPE evaluation indices in the above table, it was evident that the temperature measurement model accurately reflected the temperature of the shiitake mushroom sticks when 850 Hz was utilized as the characteristic frequency. The elevated R^2 value indicated a strong correlation between the velocity of the composite acoustic signal and the temperature of these sticks, suggesting that the model provided an excellent fit to the data. Furthermore, as discussed in Section 2.3.1, a frequency of 850 Hz offers the highest resolution for sound velocity per unit temperature. Consequently, this study selected 850 Hz as the characteristic frequency to achieve optimal accuracy in temperature measurements.

In addition, the model performed the poorest performance at 750 Hz due to the absorption of sound waves by the shiitake mushroom stick at this frequency. This absorption diminished the proportion of penetrating acoustic signals within the composite signal, thereby weakening the correlation between the velocity of the composite acoustic signal and the temperature of these mushroom sticks.

3.2. The Effect of Moisture Content of Mushroom Sticks on Temperature Measurement Effectiveness

To assess the impact of the moisture content of shiitake mushroom sticks on the data–physics hybrid drive temperature measurement model, 10 shiitake mushroom sticks were randomly selected from each of the following moisture content ranges: 45–55%, 56–66%, and 67–77%, for a total of 30 sticks. The sticks were measured using the model at each moisture content, and the temperature of the shiitake mushroom sticks was 27.24 °C. The results of the experiment are shown in Figure 12.

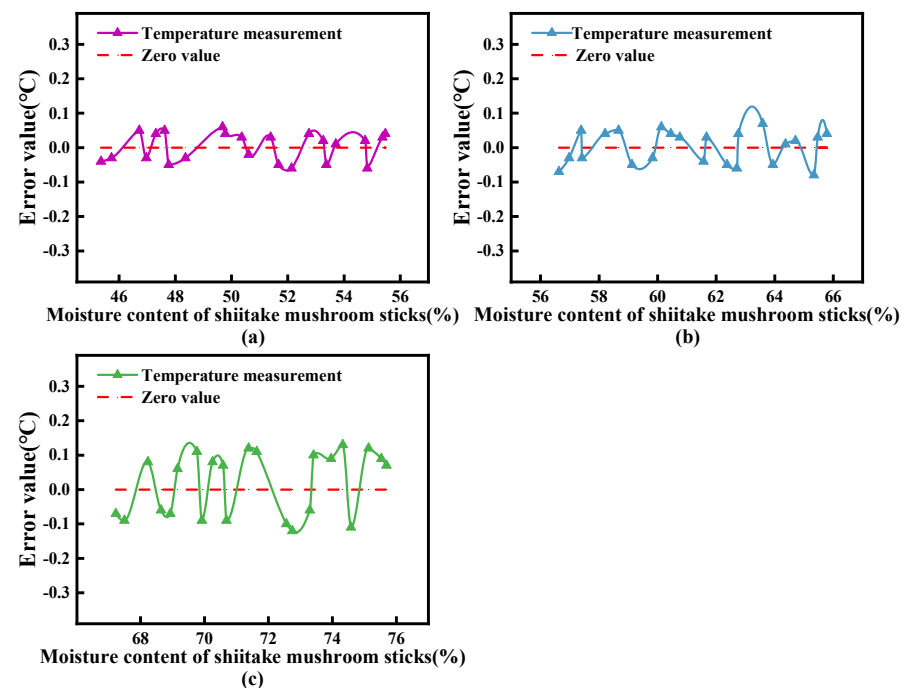


Figure 12. Temperature measurement effects of the data–physics hybrid drive model at different moisture contents in shiitake mushroom sticks. (a) Effects of moisture content in the 45–55% range

on temperature measurements of shiitake mushroom sticks; (b) Effects of moisture content in the 56–66% range on temperature measurements of shiitake mushroom sticks; (c) Effects of moisture content in the 67–77% range on temperature measurements of shiitake mushroom sticks.

In this study, W1, W2, and W3 were used to denote the moisture content intervals of 45–55%, 56–66%, and 66–77% for shiitake mushroom sticks, respectively. As shown in Figures 12 and 13, an RMSE at the 45–55% moisture content stage of the shiitake mushroom sticks was measured at 0.074 °C, with a MAE of 0.060 °C and a MAPE of 0.252%. For the 56–66% moisture content stage of the shiitake mushroom sticks, an RMSE of 0.056 °C, a MAE of 0.041 °C, and a MAPE of 0.223% were obtained. At the 66–77% moisture content stage of the shiitake mushroom sticks, an RMSE of 0.096 °C, a MAE of 0.091 °C, and a MAPE of 0.333% were obtained.

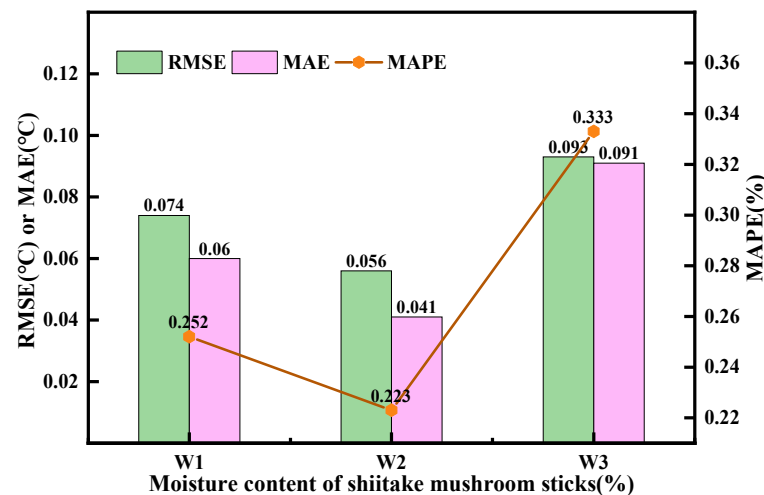


Figure 13. Model evaluation indicators for different moisture contents of shiitake mushroom sticks.

The temperature measurement model was found to perform best when the moisture content of the shiitake mushroom sticks was in the range of 56–66%; it was second best at 45–55%, and least effective at 67–77%. This variation in performance was attributed to how accurately the transmission signal from within the shiitake mushroom stick contributed to the composite signal. The moisture content was found to influence this contribution, affecting what microphone 2 received as a composite signal. As detailed in Section 2.3.3, for moisture contents of 45–55%, 56–66%, and 67–77%, the proportions of the transmission signal from shiitake mushroom sticks within the composite signal were measured at approximately 55.3%, 61.1%, and 39.51%, respectively. Notably, there was an increasing correlation between the velocity of the composite acoustic signal and temperature as this proportion rose.

3.3. Effect of Sound Source and Shiitake Mushroom Stick Spacing on Temperature Measurement Accuracy

In order to determine the optimal distance between the sound source and the shiitake mushroom sticks for model application, temperature measurements were conducted by incrementally adjusting the distance. The recorded temperature of the shiitake mushroom sticks was 26.76 °C, as shown in Figure 14.

In this paper, D1, D2, and D3 were used to denote the distance between the sound source and shiitake mushroom sticks for $x \leq 8.7$ cm, $8.7 < x \leq 16$ cm, and $16 < x \leq 30$ cm, respectively. As shown in Figure 15, within the distance range of $x \leq 8.7$ cm, the RMSE of the temperature measurement model was 0.095 °C, with a MAE of 0.085 °C and a MAPE of 0.237%. For distances in the range of $8.7 < x \leq 16$ cm, the thermometry model had an RMSE of 0.162 °C, a MAE of 0.154 °C, and a MAPE of 0.718%. In the distance range of

16 < x ≤ 30 cm, the thermometry model had an RMSE of 0.329 °C, a MAE of 0.411 °C, and a MAPE of 1.555%.

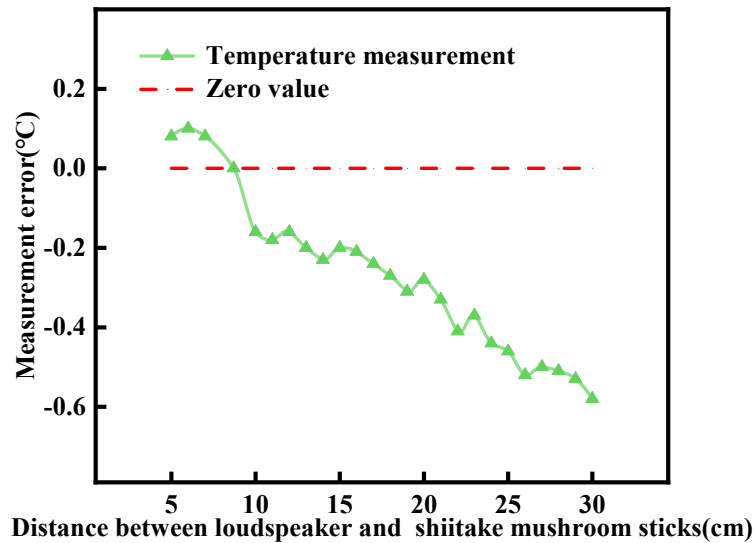


Figure 14. Measurement error in temperature attributed to the distance between the loudspeaker and the shiitake mushroom sticks.

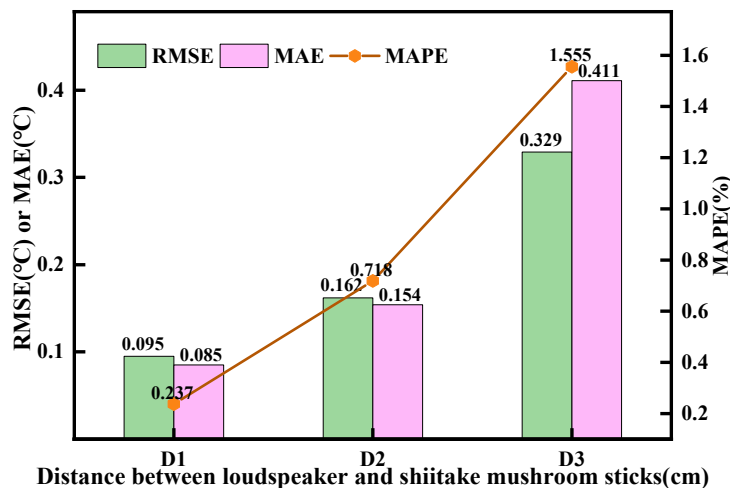


Figure 15. Evaluation indicators for models in different distance ranges between the loudspeaker and the shiitake mushroom stick.

In comparison to the range of 8.7 < x ≤ 16 cm, RMSE, MAE, and MAPE of the temperature measurement model in the range of x ≤ 8.7 cm decreased by 41.4%, 44.8%, and 66.9%, respectively. Similarly, when compared to the range of 16 < x ≤ 30 cm, RMSE, MAE, and MAPE for x ≤ 8.7 cm exhibited reductions of 50.8%, 62.5%, and 84.8%, respectively.

As the distance increased, the error in temperature measurement gradually increased. This phenomenon occurred because the increase in distance led to an increase in the proportion of the air diffraction signal in the composite signal received by microphone 2, which reduced the proportion of the shiitake mushroom stick transmission signal in the composite signal. Consequently, this resulted in a reduced correlation between the velocity of the composite acoustic signal and the temperature of the shiitake mushroom sticks. The temperature measurement error of the model was 0.08 °C at a distance of 5 cm. As the distance increased, the error changed from positive to negative. At a distance of 8.7 cm, the measured value of the model was the same as the measured value of the material temperature sensor. Therefore, the optimal distance from the sound source to the shiitake mushroom stick was 8.7 cm.

3.4. Comparing Temperature Measurement Models

Two physical constraints were employed to enhance the temperature measurement performance of the model. This paper selected a purely data-driven XGboost temperature measurement model, a model with only monotonicity constraints added to the velocity of the composite acoustic signal and the temperature of the shiitake mushroom stick; and a model with only the physical constraint being that the difference between the temperature of the shiitake mushroom stick and the air temperature was less than 2 °C added to compare with the model in this paper. The actual temperature measurement results are shown in Figure 16.

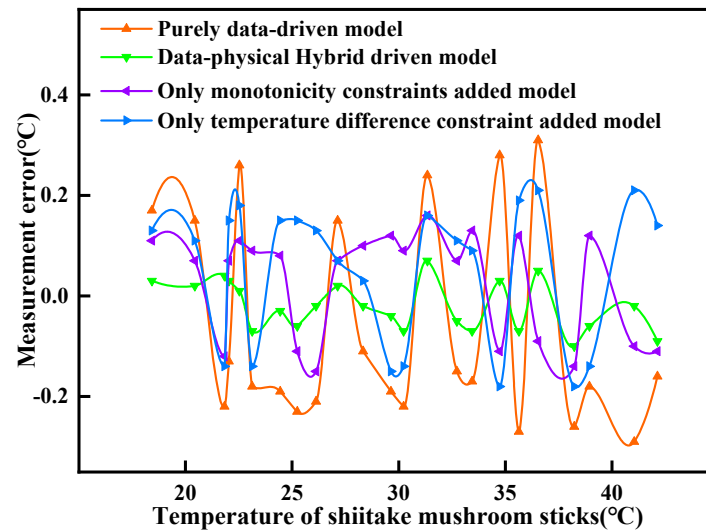


Figure 16. Comparison of the effects of temperature measurement models.

The models M1, M2, M3, and M4 depicted in Figure 17 correspond to the purely data-driven model, the model with only monotonicity constraints added, the model with only temperature difference constraints added, and the data–physics hybrid-driven model, respectively.

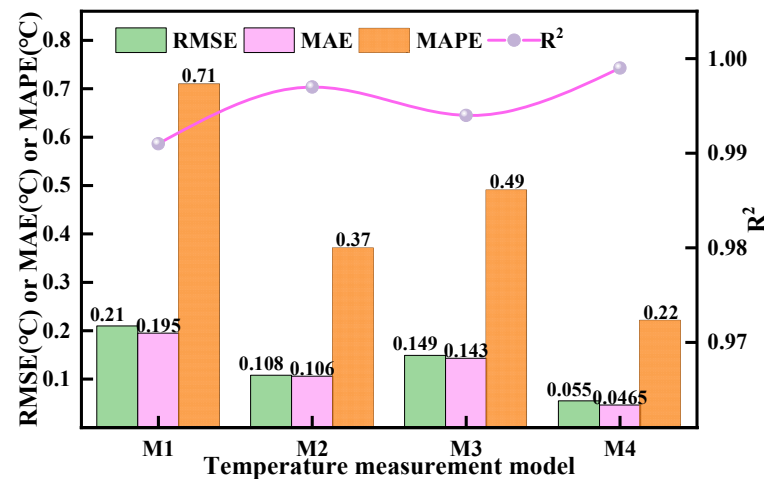


Figure 17. Evaluation indicators for different models.

The purely data-driven model M1 exhibited an RMSE of 0.21 °C, a MAE of 0.195 °C, a MAPE of 0.71%, and an R² value of 0.991. The purely data-driven model M2, which incorporated monotonicity constraints, demonstrated an RMSE of 0.108 °C, a MAE of 0.106 °C, a MAPE of 0.37%, and an R² value of 0.997. The purely data-driven model M3, also with monotonicity constraints, had an RMSE of 0.149 °C, a MAE of 0.143 °C, a MAPE

of 0.49%, and an R^2 value of 0.994. The data–physics hybrid model M4 achieved an RMSE of 0.055 °C, a MAE of 0.0465 °C, a MAPE of 0.22%, and an R^2 value of 0.999.

The comparison of the metrics indicated that the introduction of physical constraints enhanced model performance. The purely data-driven model exhibited substantial errors; however, after incorporating monotonicity constraints between the velocity of the composite acoustic signal and the temperature of the shiitake mushroom sticks, all error metrics showed significant improvement: the RMSE decreased by 48.57%, MAE decreased by 45.64%, MAPE decreased by 47.89%, and R^2 improved by 0.605%. Adding the physical constraint that limited the difference between the shiitake mushroom stick temperature and air temperature to less than 2 °C resulted in a smaller improvement compared to previous adjustments, but it still reduced errors relative to the purely data-driven model. Ultimately, the data–physics hybrid-driven model, which integrated both physical constraints, achieved remarkable enhancements: the RMSE decreased by 74.86%, MAE decreased by 77.22%, MAPE decreased by 69.30%, and R^2 improved by 0.807%. These results clearly demonstrated that introducing physical constraints significantly optimized predictive performance, with improvements becoming increasingly pronounced as more types and numbers of physical constraints were applied.

To further assess the stability of the aforementioned four models, a 5-fold cross-validation approach was employed to evaluate the temperature measurement accuracy of these four models. In this study, the training set and validation set were combined and partitioned into five equally sized subsets. At each iteration, one subset was designated as the validation set while the remaining four subsets served as the training set; notably, the test set was excluded from this cross-validation process. The specific methodology is illustrated in Figure 18.

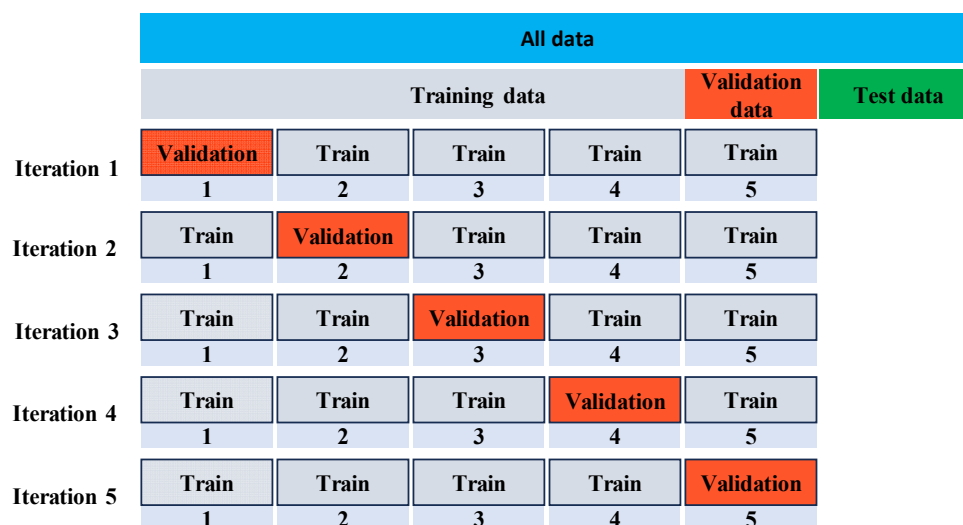


Figure 18. The 5-Fold cross-validation principle.

The accuracy of the predictions generated by the four thermometry models in each fold of the validation set is presented in Table 2 below.

Table 2. Accuracy of 5-fold cross-validation for each temperature measurement model.

Models	Iteration 1	Iteration 2	Iteration 3	Iteration 4	Iteration 5	Average Accuracy (%)
M1	92.856	93.642	93.156	94.103	92.683	93.288
M2	97.368	96.963	97.823	97.657	98.334	97.629
M3	96.753	96.145	97.263	95.961	96.393	96.503
M4	98.236	98.879	99.534	99.245	98.331	98.845

According to the results of cross-validation for each model, the purely data-driven model M1, the model incorporating only monotonicity constraints (M2), the model with solely temperature difference constraints (M3), and the data–physics hybrid-driven model (M4) exhibited commendable accuracy, with prediction accuracies of 93.288%, 97.629%, 96.503%, and 98.845%, respectively. The introduction of additional constraints significantly enhanced their predictive performance. Notably, the M4 model achieved an impressive accuracy of 98.845%, demonstrating exceptional stability and reliability in predicting temperatures based on the relationship between sound velocity and shiitake mushroom stick.

4. Discussion

This study utilized changes in sound speed to achieve non-destructive temperature measurements of shiitake mushroom sticks. When combined with the effective accumulated temperature method, this approach was found to accurately determine the physiological maturity of the mycelium in these mushroom sticks. This is of great significance for timely transitioning to the fruiting stage, enhancing mushroom yield, reducing energy consumption during industrial cultivation, and shortening the production cycle of edible fungi.

By employing the acoustic non-destructive thermometry method that was proposed in this study, corresponding embedded devices can be developed to collect essential data such as sound speed and air temperature, enabling the calculation of the internal temperature of shiitake mushroom stick using the model that was constructed herein. Regarding model applicability, the framework developed in this study is considered suitable for the cultivation stage of shiitake mushrooms and can also be applied to the cultivation environments of other edible fungi. Regarding model applicability, the framework developed in this study is considered suitable for the cultivation stage of shiitake mushrooms and can also be applied to the cultivation environments of other edible fungi, such as *Auricularia auricula* and oyster mushrooms, within bag cultivation systems. In contrast to these species, shiitake mushroom sticks are equipped with two-layer moisture-preserving bags that are designed to provide enhanced moisture retention [33]. When the model is applied to these mushrooms, the moisture content of the shiitake mushroom sticks varied relatively more in the mushroom-raising environment. Factory-cultivated mushroom rooms, such as those for shiitake mushrooms, are usually well equipped, with better facility conditions, such as air conditioning units and fresh air units, which can effectively regulate the climate in the mushroom-raising room [34]. The fruiting process of shiitake mushrooms occurs in plastic greenhouses in southern China and sun greenhouses in northern China [35]. The common feature of such facilities is that they are heavily dependent on natural weather conditions, and the environmental control equipment is weak in regulating and controlling the conditions, making it impossible to accurately control conditions of air temperature and air humidity. Therefore, the influencing factors to be considered in applying the model constructed in this paper to shiitake mushrooms and other mushrooming processes will be increased.

5. Conclusions

This study proposed a method for measuring the internal temperature of shiitake mushroom sticks utilizing acoustic sensors. The method began by collecting sound velocity data at various acoustic frequencies, along with measurements of moisture content and the temperatures of the shiitake mushroom sticks through multiple experimental setups. Subsequently, a temperature measurement model was constructed based on the XGBoost algorithm, utilizing sound velocity, air temperature, and moisture content as inputs while predicting the temperature of the shiitake mushroom stick as outputs. This approach incorporated monotonicity constraints between the shiitake mushroom stick's temperature, sound velocity, and constraints, ensuring that the difference between the shiitake mushroom stick temperature and air temperature remained below 2 °C. The results indicated that at an acoustic frequency of 850 Hz, with the moisture content in the range of 56–66% and

a distance from the sound source to the mushroom stick set at 8.7 cm, the data–physics hybrid-driven model presented in this paper achieved reductions in RMSE, MAE, and MAPE by 74.86%, 77.22%, and 69.30%, respectively; additionally, it enhanced the R^2 value by 1.86% compared to a purely data-driven temperature measurement model.

Future research will incorporate sweeping and imaging technologies, aiming to further investigate the velocity temperature relationship model across various eigenfrequencies. This effort seeks to enhance the accuracy of temperature measurements for shiitake mushroom sticks and facilitate the visualization of temperature field distribution. Additionally, we plan to develop an embedded system that integrates data acquisition, processing, and analysis functions while reducing equipment size to enable networked or portable monitoring capabilities.

Author Contributions: Conceptualization, X.Z. (Xin Zhang) and X.Z. (Xinwen Zeng); methodology, X.Z. (Xin Zhang) and X.Z. (Xinwen Zeng); software, X.Z. (Xinwen Zeng); validation, X.Z. (Xin Zhang), W.Z. and M.W.; formal analysis, Y.W.; resources, M.W.; data curation, X.Z. (Xin Zhang) and M.W.; writing—original draft preparation, X.Z. (Xin Zhang) and X.Z. (Xinwen Zeng); writing—review and editing, X.Z. (Xin Zhang), Y.W. and W.Z.; visualization, X.Z. (Xinwen Zeng); supervision, W.Z.; funding acquisition, Y.W. and M.W. All authors have read and agreed to the published version of the manuscript.

Funding: The APC was funded by the Beijing Academy of Agricultural and Forestry Sciences Science and Technology Innovation Capacity Construction Project (KJCX20230410), the China Agriculture Research System of MOF and MARA (CARS-20), and the Beijing edible fungi Innovation Team (BAIC03-2024).

Institutional Review Board Statement: The study did not require ethical approval.

Data Availability Statement: We have committed to providing all relevant data promptly upon the official publication of the article and ensuring that the data are accessible in accordance with the journal’s requirements. Thank you for your understanding and support. For further information about the data, please contact Dr. Mingfei Wang at wangmf@nercita.org.cn.

Acknowledgments: The authors would like to thank the anonymous reviewers for their constructive comments, which helped improve the quality of this paper.

Conflicts of Interest: The authors declare no conflicts of interest.

References

1. Safaie, N.; Salehi, M.; Farhadi, S.; Aligholizadeh, A.; Mahdizadeh, V. *Lentinula edodes* substrate formulation using multilayer perceptron-genetic algorithm: A critical production checkpoint. *Front. Microbiol.* **2024**, *15*, 1366264. [[CrossRef](#)]
2. Royse, D.J.; Schisler, L.C.; Diehle, D.A. Shiitake mushrooms consumption, production and cultivation. *Interdiscip. Sci. Rev.* **1985**, *10*, 329–335. [[CrossRef](#)]
3. Hu, Y.; Xue, F.; Chen, Y.; Qi, Y.; Zhu, W.; Wang, F.; Shen, J. Effects and Mechanism of the Mycelial Culture Temperature on the Growth and Development of *Pleurotus ostreatus* (Jacq.) P. Kumm. *Horticulturae* **2023**, *9*, 95. [[CrossRef](#)]
4. Zhang, J.; Tang, B.; Hu, S. Infrared and visible image fusion based on particle swarm optimization and dense block. *Front. Energy Res.* **2022**, *10*, 1001450. [[CrossRef](#)]
5. Guo, J.; Shang, H.; Cai, G.; Wang, K.; Li, S. Early detection of coal spontaneous combustion by complex acoustic waves in a concealed fire source. *ACS Omega* **2023**, *8*, 16519–16531. [[CrossRef](#)]
6. Guo, J.; Gao, W.; Cai, G.; Liu, Y.; Wang, K. Acoustic temperature measurement of loose coals based on pseudo-random sequences and application research. *Coal Sci. Technol.* **2024**, *52*, 123–131.
7. Guo, M.; Shang, Z.Y.; Shi, H.W. A study of the sound absorption property of grain. *J. Appl. Sci.* **2003**, *2*, 111–116.
8. Othmani, C.; Taktak, M.; Zein, A.; Hentati, T.; Elnady, T.; Fakhfakh, T.; Haddar, M. Experimental and theoretical investigation of the acoustic performance of sugarcane wastes based material. *Appl. Acoust.* **2016**, *109*, 90–96. [[CrossRef](#)]
9. Guo, M.; Yan, Y.; Hu, Y.; Lu, G.; Zhang, J. Temperature measurement of stored biomass using low-frequency acoustic waves and correlation signal processing techniques. *Fuel* **2018**, *227*, 89–98. [[CrossRef](#)]
10. Hu, Y.; Guo, M.; Yan, Y.; Lu, G.; Cheng, X. Temperature measurement of stored biomass of different types and bulk densities using acoustic techniques. *Fuel* **2019**, *257*, 115986. [[CrossRef](#)]
11. Ostashev, V.E.; Vecherin, S.N.; Wilson, D.K.; Ziemann, A.; Goedecke, G.H. Recent progress in acoustic travel-time tomography of the atmospheric surface layer. *US Army Res.* **2009**, *18*, 125–133. [[CrossRef](#)]

12. Barth, M.; Raabe, A. Acoustic tomographic imaging of temperature and flow fields in air. *Meas. Sci. Technol.* **2011**, *22*, 035102. [[CrossRef](#)]
13. Guo, M.; Yan, Y.; Lu, G.; Hu, Y.H. Research on air temperature measurement using low frequency sound waves. *Chin. J. Sci. Instrum.* **2018**, *39*, 76–82.
14. Yan, H.; Chen, G.; Zhou, Y.; Liu, L. Primary study of temperature distribution measurement in stored grain based on acoustic tomography. *Exp. Therm. Fluid Sci.* **2012**, *42*, 55–63. [[CrossRef](#)]
15. Guo, M.; Hu, Y. Measurement of sound travel time in stored bulk material using cross-correlation techniques. *J. Electron. Meas. Instrum.* **2018**, *32*, 6–14.
16. Holstein, P.; Raabe, A.; Müller, R.; Barth, M.; Mackenzie, D.; Starke, E. Acoustic tomography on the basis of travel-time measurement. *Meas. Sci. Technol.* **2004**, *15*, 1420. [[CrossRef](#)]
17. Bao, Y.; Jia, J.; Polydorides, N. Real-time temperature field measurement based on acoustic tomography. *Meas. Sci. Technol.* **2017**, *28*, 074002. [[CrossRef](#)]
18. Lin, F.S.; Pal, S.; Lu, C.Y.; Du, S.W.; Huang, M.C.; Wu, C.H.; Huang, C.H. Reconstructing 2-D gas temperature distribution with deep neural networks. *IEEE Sens. J.* **2022**, *23*, 2891–2899. [[CrossRef](#)]
19. Zhong, Q.; Chen, Y.; Zhu, B.; Liao, S.; Shi, K. A temperature field reconstruction method based on acoustic thermometry. *Measurement* **2022**, *200*, 111642. [[CrossRef](#)]
20. Jeong, J.; Lee, J.; Sun, H.; Park, H.; Kim, S.; Bak, M.S. Temperature field estimation of an axisymmetric laminar flame via time-of-arrival measurements of acoustic waves, and machine learning. *Exp. Therm. Fluid Sci.* **2021**, *129*, 110454. [[CrossRef](#)]
21. Ma, T.; Liu, Y.; Cao, C. Neural networks for 3D temperature field reconstruction via acoustic signals. *Mech. Syst. Signal Process.* **2019**, *126*, 392–406. [[CrossRef](#)]
22. Jeon, Y.J.; Kim, J.Y.; Hwang, K.S.; Cho, W.J.; Kim, H.J.; Jung, D.H. Machine Learning-Powered Forecasting of Climate Conditions in Smart Greenhouse Containing Netted Melons. *Agronomy* **2024**, *14*, 1070. [[CrossRef](#)]
23. Tang, J.; Liu, K.; You, W.; Zhang, X.; Zhang, T. Research on Online Temperature Prediction Method for Office Building Interiors Based on Data Mining. *Energies* **2023**, *16*, 5570. [[CrossRef](#)]
24. Weierbach, H.; Lima, A.R.; Willard, J.D.; Hendrix, V.C.; Christianson, D.S.; Lubich, M.; Varadharajan, C. Stream temperature predictions for river basin management in the Pacific Northwest and mid-Atlantic regions using machine learning. *Water* **2022**, *14*, 1032. [[CrossRef](#)]
25. Yang, J.W.; Dashdondov, K. In-Depth Examination of Machine Learning Models for the Prediction of Ground Temperature at Various Depths. *Atmosphere* **2022**, *14*, 68. [[CrossRef](#)]
26. Wang, M.; Kong, X.; Shan, F.; Zheng, W.; Ren, P.; Wang, J.; Zhao, C. Temperature Prediction of Mushrooms Based on a Data—Physics Hybrid Approach. *Agriculture* **2024**, *14*, 145. [[CrossRef](#)]
27. Das, P.; Jha, G.K.; Lama, A.; Parsad, R. Crop yield prediction using hybrid machine learning approach: A case study of lentil (*Lens culinaris* Medik.). *Agriculture* **2023**, *13*, 596. [[CrossRef](#)]
28. Ufimtsev, P.Y.; Apaydin, G.; Sevgi, L. Shadow radiation and Fresnel diffraction of acoustic waves. *J. Acoust. Soc. Am.* **2022**, *151*, 4063–4072. [[CrossRef](#)]
29. Skobel'syn, S.A.; Tolokonnikov, L.A. Sound diffraction on a sphere with an inhomogeneous coating in a plane waveguide. *Mech. Solids* **2020**, *55*, 1351–1362. [[CrossRef](#)]
30. Zubov, Y.; Djafari-Rouhani, B.; Sofield, M.; Walker, E.; Neogi, A.; Krokhin, A. Long-range nonspreading propagation of sound beam through periodic layered structure. *Commun. Phys.* **2020**, *3*, 155. [[CrossRef](#)]
31. Li, L.T.; He, C.F.; Wu, B. Research on restraining dispersive characteristics of ultrasonic guided wave in a long pipe. *J. Data Acquis. Process.* **2004**, *19*, 297–301.
32. Trang, N.T.H.; Thuy, N.T.B.; Mo, N.T.; Luyen, N.T.; Nghien, N.X. Optimal Culture Conditions for the Enhanced Mycelial Growth and Cultivation of Shiitake Mushroom (*Lentinula edodes*): Optimal culture conditions for the enhanced mycelial growth and cultivation of shiitake mushroom. *Vietnam J. Agric. Sci.* **2023**, *6*, 1958–1968.
33. Jhune, C.S.; Kong, W.S.; Park, H.S.; Cho, J.H.; Lee, K.H. Mushroom growth and cultivation environment at cultivation house of vinyl bag cultivation Shiitake mushroom on high-temperature period. *J. Mushroom* **2014**, *12*, 263–269. [[CrossRef](#)]
34. Chen, L.; Qian, L.; Zhang, X.; Li, J.; Zhang, Z.; Chen, X. Research progress on indoor environment of mushroom factory. *Int. J. Agric. Biol. Eng.* **2022**, *15*, 25–32. [[CrossRef](#)]
35. Wang, M.; Zheng, W.; Zhao, C.; Chen, Y.; Chen, C.; Zhang, X. Energy-Saving Control Method for Factory Mushroom Room Air Conditioning Based on MPC. *Energies* **2023**, *16*, 7623. [[CrossRef](#)]

Disclaimer/Publisher's Note: The statements, opinions and data contained in all publications are solely those of the individual author(s) and contributor(s) and not of MDPI and/or the editor(s). MDPI and/or the editor(s) disclaim responsibility for any injury to people or property resulting from any ideas, methods, instructions or products referred to in the content.